A Novel Trajectory Restoration Algorithm for High-Resolution SAR Imaging

Ievgen M. Gorovyi, Oleksandr O. Bezvesilniy and Dmytro M. Vavriv
Department of Microwave Electronics, Institute of Radio Astronomy of NAS of Ukraine
4 Chervonopraporna Str., Kharkov 61002, Ukraine
gorovoy@rian.kharkov.ua, obezv@rian.kharkov.ua, vavriv@rian.kharkov.ua

Abstract— **The quality of high-resolution SAR imaging is strictly related with the precision of the platform trajectory measurements. This is one of the crucial points in the case of image formation from light-weight aircrafts and UAV platforms, which undergone significant trajectory instabilities in real flight conditions. In the paper, a new approach for the residual range-dependent phase error restoration is proposed. According to the method, the cross-track aircraft accelerations are evaluated via a specifically developed weighted estimation procedure. The reconstructed residual trajectory deviations are used for the range-dependent motion errors compensation. The corresponding experimental results are also demonstrated.**

Keywords—synthetic aperture radar; autofocusing; SAR processing; motion errors; residual trajectory deviations

I. INTRODUCTION

High-quality imaging with synthetic aperture radars (SAR) implies precise trajectory measurements [1]-[5]. The problem is that even modern navigation systems often do not fulfill the accuracy requirements. The common solution in this case is the application of autofocusing methods.

The aim of any autofocusing approach is the extraction of the residual (unknown and, therefore, uncompensated) phase error function directly from the radar raw data. One of the most known methods is the map-drift autofocus (MDA) [5]-[8]. Its idea is related with the estimation of the shift between two SAR looks for the unknown quadratic phase error determination. Recently, it has been shown that the estimation of the local quadratic phase errors can be used for the reconstruction of an arbitrary phase error function [7].

However, the problem of accounting for the phase error range dependence is still a challenge. This is especially critical for a low altitude and squinted SAR, when the phase error demonstrates strong range dependence.

In the paper, the idea of the restoration of the residual platform deviations is described. The method is based on an independent processing of small azimuth data blocks for the estimation of local quadratic phase errors (and the related local Doppler rate errors). Such estimates are also performed independently for a number of range blocks across the swath. These local estimates are used for the evaluation of the residual cross-track components of the aircraft acceleration. An efficient weighting scheme is proposed for such restoration that allows to retrieve the unknown trajectory deviations more precisely. Thus, an arbitrary time-dependent and range-dependent phase error function can be reconstructed. The approach does not require the presence of bright points on the scene and can be used in both the stripmap and spotlight SAR modes.

In Section II, the principle of the local phase error estimation is described. In particular, the aperture synthesis on a short-time interval and peculiarities of calculation of local correlation between the pair of SAR images are considered. The method for the evaluation of the residual deviations using the weighted estimation is considered in Section III. Examples of real SAR images obtained with the X-band SAR system [9] are given in Section IV.

II. LOCAL PHASE ERROR ESTIMATION

In general, the presented residual phase error is an arbitrary function $\varphi(R,t)$. It has been shown [7], [10] that it is possible to introduce short-time intervals T_S and apply a local approximation to the segments of the phase error function on each interval as follows:

$$\varphi_E(R,t_n+\tau) \approx \varphi_E(R,t_n) + \varphi'_E(R,t_n)\tau + \varphi''_E(R,t_n)\tau^2/2,$$

where R is a particular range gate, t_n is the center of the considered short-time interval, τ is the time within the short interval, $-T_S/2 < \tau < T_S/2$. It is known that the linear phase term $\varphi'_E(R,t_n)\tau$ leads to a shift of the SAR image in the azimuth direction, the quadratic phase error term $\varphi''_E(R,t_n)\tau^2/2$ results in defocusing, while the constant term $\varphi_E(R,t_n)$ does not affect the aperture synthesis. On the one hand, the lengths of such short intervals should be chosen to provide a sufficient precision of this parabolic phase error approximation. On the other hand, the interval length should be increased iteratively up to the length of synthesis required to achieve the desired high azimuth resolution on the final SAR image.

The first step before the local estimation is the formation of the pair of SAR images on two halves of the above considered short-time interval. The common way to do this is to apply the range-Doppler algorithm specifically modified

for such SAR processing [7]. According to this method, the images can be obtained as follows:

$$I_{1,2}(t) = \int_{-\Delta F_A/2}^{\Delta F_A/2} S_{1,2}(f) H^*(f) \exp[2\pi i f t] df \ ,$$

where ΔF_A is the Doppler spectrum bandwidth corresponding to the antenna beam width in the azimuth direction, $S_{1,2}(f)$ are the spectra calculated from the halves of the short-time interval data:

$$S_1(f) = \frac{2}{T_S} \int_{-T_S/2}^{0} w_S(\tau + T_S/4) s(\tau) \exp[-2\pi i f \tau] d\tau \ ,$$

$$S_2(f) = \frac{2}{T_S} \int_{0}^{T_S/2} w_S(\tau - T_S/4) s(\tau) \exp[-2\pi i f \tau] d\tau \ .$$

The spectrum of the reference function is calculated as follows:

$$H(f) = \int_{-T_A/2}^{T_A/2} w_H(t) h(t) \exp[-2\pi i f t] dt \ .$$

Here T_A is the maximum time of the synthesis limited in the stripmap mode by the size of the antenna footprint, $w_S(\tau)$ and $w_H(t)$ are the weighting windows, which should be applied in the time domain, $h(t)$ is the reference function:

$$h(t) = \exp[2\pi i (F_{DC} t + F_{DR} t^2/2)] \ ,$$

F_{DC} and F_{DR} are the known Doppler centroid and Doppler rate.

The described above convolution-based SAR image synthesis requires the azimuth sampling frequency to be sufficient in order to represent the whole Doppler bandwidth. Only in this case one can perform unambiguous sampling of the long reference function (on the interval T_A), which is convolved with signals on the short intervals $T_S/2$. Evidently, such convolution-based method requires a lot of computations.

In order to reduce the number of computations, the dechirp method [5], [11]-[12] can be used for the SAR image formation on the short-time intervals. According to this technique the pair of images can be obtained as follows:

$$I_1(f) = \frac{2}{T_S} \int_{-T_S/2}^{0} w_S(\tau + T_S/4) s(\tau) h^*(\tau) \exp[-2\pi i f \tau] d\tau \ ,$$

$$I_2(f) = \frac{2}{T_S} \int_{0}^{T_S/2} w_S(\tau - T_S/4) s(\tau) h^*(\tau) \exp[-2\pi i f \tau] d\tau \ .$$

As the result, one can form the SAR image from each half-interval by using a single short Fourier transform.

In the case of the presence of a local quadratic phase error, the SAR images will be defocused and shifted in the azimuth in the opposite directions. The shift can be determined from the following equation:

$$\Delta f_{\max} = f_{1\max} - f_{2\max} = F_{DR}^E T_S / 2 \ .$$

The common way to measure the shift is to calculate a cross-correlation function of the pair of SAR images. For a particular range gate it is determined as

$$R_{CC}(R, \Delta f) = \int |I_1(R, f)|^2 |I_2(R, f + \Delta f)|^2 \ df \ .$$

The position of the cross-correlation peak should be measured precisely in order to obtain a good estimate of the local Doppler rate error F_{DR}^E. One should notice that the efficiency of such measurement significantly depends on the images content. In particular, the low image contrast can lead to inaccurate estimation of the peak position. In order to improve the estimation quality, several preprocessing steps should be performed (Fig. 1). At first, the images are recalculated into a logarithmic scale and the dynamic range is narrowed. This allows to balance contributions from bright and dark image features. After that, the local centering is performed, enhancing the local contrast of image details and significantly narrowing the correlation peaks. The image preprocessing significantly improves the precision of the peak position estimation.

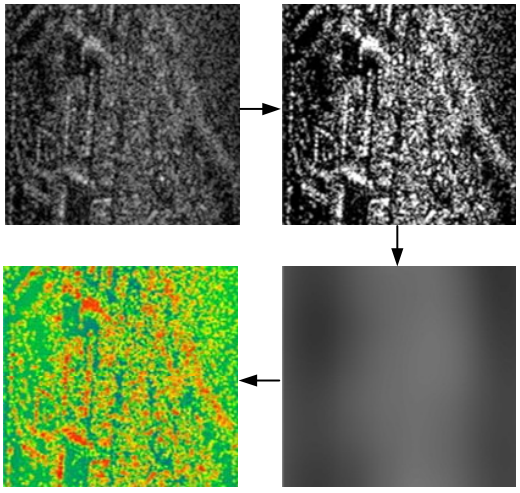

Figure 1. SAR images preprocessing steps.

As the result of the described local estimations, values of the Doppler rate errors are obtained. In the next section, the principle of the reconstruction of the residual trajectory deviations by using the obtained local estimates is described.

III. Weighting Scheme and Residual Deviations

The range dependence of the residual phase error function is one of the crucial points, especially for low-altitude and wide-range-swath SAR systems. In order to perform the estimation of the range-dependent residual phase error, the method for the evaluation of the residual trajectory deviations is proposed.

One can show that the Doppler rate of the backscattered signal is determined as follows:

$$F_{DR}(R,t_n) = \\ = -\frac{2}{\lambda}\left[\frac{1}{R}\left(\left|\vec{V}+\vec{v}_E(t_n)\right|^2 - \left(\frac{\vec{R}\cdot\left(\vec{V}+\vec{v}_E(t_n)\right)}{R}\right)^2\right) - \frac{\vec{R}\cdot\vec{a}_E(t_n)}{R}\right],$$

where $\vec{v}_E(t_n)$ is the residual velocity error vector, $\vec{a}_E(t_n)$ is the residual acceleration vector, $\vec{R}(x_R, y_R, -H)$ is the slant range vector, and

$$x_R = H\tan\alpha\cos\beta + \sin\beta\sqrt{R^2 - H^2 - (H\tan\alpha)^2},$$
$$y_R = -H\tan\alpha\sin\beta + \cos\beta\sqrt{R^2 - H^2 - (H\tan\alpha)^2}$$

are the coordinates on the Doppler centroid line, R is the slant range, α, β are the antenna pitch and yaw angles, respectively.

One can see that the residual Doppler rate error F_{DR}^E depends on the residual velocity error and the residual acceleration that are left uncompensated because of inaccuracies of the trajectory measurements. It has been found that the main contribution to these errors is related with the cross-track acceleration components. Therefore, the estimated Doppler rate error can be written as

$$F_{DR}^E(R,t_n) \approx \frac{2}{\lambda}\frac{y_R a_Y(t_n) - H a_Z(t_n)}{R}.$$

This equation can be used to evaluate the unknown cross-track acceleration components. For this purpose, the local estimation of Doppler rate errors should be performed within several range blocks. In this case, a series of the local estimates $\left(R_m, F_{DR}^E(R_m)\right)$ will be obtained. Here R_m corresponds to the central range gate within the range block. In order to perform the described estimation, the mean square error (MSE) estimator is constructed:

$$MSE(a_Y(t_n), a_Z(t_n)) = \\ = \sum_{m=1}^{M_R} w_m \left[\frac{2}{\lambda}\frac{y_{R_m} a_Y(t_n) - H a_Z(t_n)}{R_m} - F_{DR}^E(R_m, t_n)\right]^2,$$

where w_m are weighting coefficients which are determined as values of the cross-correlation functions maxima. Such choice can be justified. The value of the cross-correlation peak is proportional to the image contrast. The higher the contrast of the range block the better is the estimation precision, and vice versa. Therefore, such weighting improves the overall performance of the MSE scheme and leads to a more precise cross-track acceleration evaluation.

An example of the local correlation functions $R_{CC}(m, \Delta x)$ for all range blocks is illustrated in Fig. 2. One can see that the maximum values of the cross-correlation peaks are changed for different range blocks.

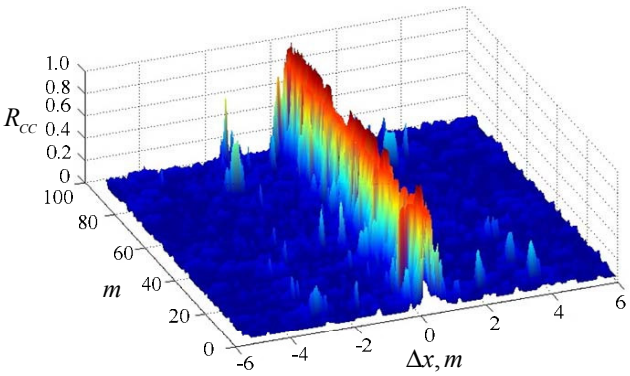

Figure 2. Cross-correlation functions for different range blocks.

Using the above defined MSE estimator, the resulting system of equations can be written as follows:

$$a_Y(t_n)\sum_{m=1}^{M_R} w_m\left(\frac{y_{R_m}}{R_m}\right)^2 - a_Z(t_n)\sum_{m=1}^{M_R} w_m\left(\frac{y_{R_m}}{R_m}\frac{H}{R_m}\right) = \\ = \frac{\lambda}{2}\sum_{m=1}^{M_R} w_m F_{DR}^E(R_m, t_n)\frac{y_{R_m}}{R_m},$$

$$a_Y(t_n)\sum_{m=1}^{M_R} w_m\left(\frac{y_{R_m}}{R_m}\frac{H}{R_m}\right) - a_Z(t_n)\sum_{m=1}^{M_R} w_m\left(\frac{H}{R_m}\right)^2 = \\ = \frac{\lambda}{2}\sum_{m=1}^{M_R} w_m F_{DR}^E(R_m, t_n)\frac{H}{R_m}.$$

The solutions of the above system of equations for the sequence of short-time intervals t_n give the time series of the cross-track acceleration components $a_Y(t_n), a_Z(t_n)$. At the next step, the residual trajectory deviations are reconstructed by double integration, and then can be used for the calculation of the range-dependent phase error function. Finally, the estimated residual phase error is compensated in the SAR data.

IV. Experimental Results

In this section, the main steps of the developed autofocusing approach are described, and examples of experimental results are demonstrated.

The input for the autofocus algorithm is the SAR data after the conventional steps including the range compression, the range cell migration correction, and also the motion compensation procedure based on the trajectory measurements. The obtained data buffer is ready for the application of the developed autofocus technique.

The main stages of the proposed method are shown in Fig. 3. At the first step, the raw data are divided on small azimuth blocks, which correspond to the short-time intervals. After that, the pairs of SAR images are built with the dechirp algorithm. The obtained images are then divided into the range blocks for the independent Doppler rate errors estimation.

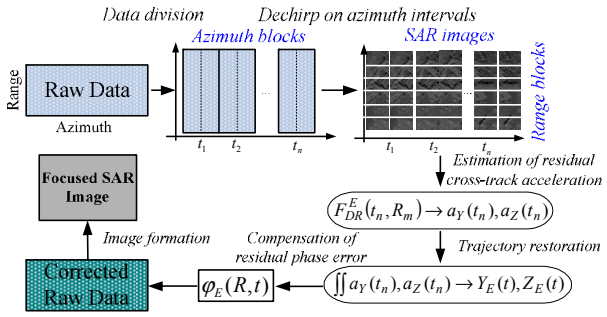

Figure 3. Block-scheme of the proposed algorithm.

These errors are used for the cross-track acceleration $a_Y(t_n), a_Z(t_n)$ reconstruction for each of the short-time intervals. At the next step, the residual trajectory deviations are obtained via double integration. Finally, the range-dependent residual phase error function is calculated and compensated in the SAR data.

The proposed autofocusing approach has been tested with the airborne RIAN-SAR-X system [9] developed and produced at the Institute of Radio Astronomy of the National Academy of Sciences of Ukraine.

A multi-look SAR image with 25 looks and a 2-m resolution built without autofocusing is shown in Fig. 4a.

(a)

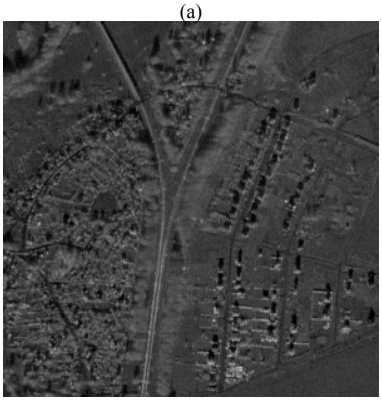

(b)

Figure 4. Multi-look SAR images (25 looks, 2-m resolution): (a) – before autofocusing, (b) – after autofocusing.

One can observe significant defocusing, which is the result of the existence of residual phase errors. The SAR image of the same scene after the application of the developed autofocusing approach is shown in Fig. 4b. This image is well focused what demonstrates the efficiency of the proposed autofocus technique.

V. Conclusion

In the paper, a novel approach for the estimation of an arbitrary residual phase error from SAR data is developed. The method uses the local estimates of the Doppler rate errors on short-time intervals and for a number of range blocks for the cross-track acceleration evaluation. The obtained time series of the cross-track acceleration components is used for the reconstruction of the residual trajectory deviations. The main advantage of the method is the ability to handle both time-varying and range-dependent phase errors. This method is especially useful for SAR systems operated from light-weight aircrafts and UAV platforms. The performed analysis of experimental data demonstrates a high performance of the developed approach.

References

[1] V.C. Koo at al. "A New Unmanned Aerial Vehicle Synthetic Aperture Radar for Environmental Monitoring", Progress In Electromagnetics Research, Vol. 122, pp. 245-268, 2012.

[2] S. Stanko at al., "SUMATRA – A UAV based miniaturized SAR System", Proc. on 9th Synthetic Aperture Radar Conference,pp. 437-440, 2012.

[3] C. Oliver and S. Quegan, Understanding Synthetic Aperture Radar Images. Norwood, MA: Artech House, 1999.

[4] G. Franceschetti and R. Lanari, Synthetic Aperture Radar Processing. CRC Press, 1999.

[5] W. G. Carrara, R. S. Goodman, and R. M. Majewski, Spotlight Synthetic Aperture Radar: Signal Processing Algorithms. Boston; London: Artech House, 1995.

[6] P. Samczynski and K. Kulpa, "Coherent MapDrift technique", IEEE Trans. on Geoscience and Remote Sensing, vol. 48, no. 3, pp. 1505–1517, March 2010.

[7] O.O. Bezvesilniy, I.M. Gorovyi and D.M. Vavriv, "Estimation of phase errors in SAR data by local-quadratic map-drift autofocus", Proc. 13th Int. Radar Symp. IRS-2012, Warsaw, Poland, pp. 376-381, 2012.

[8] H. M. J. Cantalloube and C. E. Nahum, "Multiscale local map-drift-driven multilateration SAR autofocus using fast polar format algorithm image synthesis", IEEE Trans. on Geoscience and Remote Sensing, vol. 49, no. 10, pp. 3730–3736, Oct 2010.

[9] D. M. Vavriv at al., "SAR Systems for Light-Weight Aircrafts", Proc. 2011 Microwaves, Radar and Remote Sensing Symp. MRRS 2011 (Kiev, Ukraine), pp. 15–19, 2011.

[10] O.O. Bezvesilniy, I.M. Gorovyi and D.M. Vavriv, "Effects of local phase errors in multi-look SAR images", Progress In Electromagnetics Research B, Vol. 53, pp.1-24, 2013.

[11] I. G. Cumming and F. H. Wong, Digital Processing of Synthetic Aperture Radar Data: Algorithms and Implementation". Norwood, MA: Artech House, 2005.

[12] J. Wang, D. Cai and Y. Wen., "Comparison of matched filter and dechirp processing used in Linear Frequency Modulation", IEEE International Conference on Computing, Control and Industrial Engineering , Vol. 2, pp. 70-73, 2011.